



DFT Study of Lithium, Sodium and Potassium salts of Amino Acids; Global Reactivity Descriptors, Optimized Parameters and Hydration Free Energy

MAHENDRA BAPURAO DHANDE¹, G KRISHNA CHAITANYA²,
DIPAK TUKARAM TAYADE³ and PAVAN VIJAY RAUT^{4*}

¹Department of Chemistry, HPTArts and RYK Science College, Nashik-422005, India.

²School of Chemical Sciences, SRTM University, Nanded-431 606, India.

³Department of Chemistry, Government Vidarbha Institute of Science and Humanities, 444604, Amravati, India.

⁴Department Of Chemistry, Smt. Radhabai Sarda Arts, Commerce & Science College Anjangaon Surji, Dist. Amravati, Pin 444705 (MH) India.

*Corresponding author E-mail: pavanraut523@gmail.com

<http://dx.doi.org/10.13005/ojc/390528>

(Received: May 03, 2023; Accepted: September 16, 2023)

ABSTRACT

A promising solvent for removing CO₂ from flue gases after combustion is aqueous solutions of amino acid salts of alkali metals. Their computational work would be extremely significant in this area. Amino acid salts of alkali metals are being explored in aqueous solutions for post-combustion CO₂ capture from flue gases. In this regard, their computational study would be of the utmost importance. The hydration free energies, total dipole moment, HOMO/LUMO band gap energy, C=O vibration of the -COOH group, bond lengths and bond angles for lithium, sodium and potassium cysteinate and prolinatate were computed in the current work using the Gaussian 09 program. Study shows that the hydration free energy for potassium salts is less than that of corresponding lithium and sodium salts. From result it could be stated that the change of alkali metal (Na/K) in amino acid salts are changing the physical structural and vibrational characteristics of amino acid salts. This study would be helpful for their evaluation as a CO₂ capturing agent.

Keywords: DFT, CO₂, Hydration free energies, Total dipole moment.

INTRODUCTION

Major greenhouse gas carbon dioxide (CO₂) is accountable for the global warming that has been observed over the past few decades, as well as for the worries about related climate change and its potential impact on humanity. Consequently,

the removal of CO₂ from a process gas is a crucial step in many industrial processes. Prior to the flue gas being released into the atmosphere, CO₂ is separated from the flue gas using CO₂ capture methods. Many researchers have examined the responses of the amino acid salt solution with CO₂¹⁻³, which is developing into a CO₂ capture absorbent.



$$\eta = \frac{I - A}{2}$$

$$\mu = -\frac{I + A}{2}$$

$$\chi = \frac{I + A}{2}$$

$$S = \frac{1}{\eta}$$

Where, I denotes the ionisation potential and A is the electron affinity. HOMO and LUMO orbital energies can be used to express I and A as $I = -E_{\text{HOMO}}$ and $A = -E_{\text{LUMO}}$ ¹⁵.

Resistance to changes in electronic configuration of a chemical species is evaluated by their chemical hardness¹⁶⁻¹⁸. It also has some important applications in topics like complex stability, chemical reactivity¹⁹, solubility of molecules and in estimation of formed product of the reaction²⁰. Calculated values of ionization product, electron affinity, hardness, potential and softness for Li-cyst, Na-cyst, K-cyst, Li-pro, Na-pro and K-pro, are presented in Table 2. Hardness and softness can also have an impact on a molecule's stability²¹. In the gaseous and aqueous phases, the chemical hardness and electronegativity values of K-AAS are marginally lower than those of corresponding Na-AAS and for Na-AAS, they are marginally lower than those of corresponding Li-AAS. The only exception is for the value for Na-AAS in the gaseous phase. Cyst-salt values are higher than pro-salt readings. All of the examined AAS experience an increase in and a decrease in electronegativity as they transition from a gaseous to an aqueous solution.

It is clear from the information in Tables 2 that the value for Li-cyst is maximum in both the aqueous phase and the gas phase.

The combined molecular properties data for the studied structures Na-gly, Na-ala, Na-val, Na-leu, K-gly, K-ala, K-val, and K-leu indicate that:

1. Chemical hardness and chemical potential values are higher in aqueous phase as compared to gas phase; whereas, softness and electronegativity show lower values for all studied structures.
2. Li-AAS, Na-AAS, and K-AAS have been shown to have the following observed trends for η and χ .

$$\eta_{\text{cyst-salt}} < \eta_{\text{pro-salt}}$$

$$\eta_{\text{Li-salt}} > \eta_{\text{Na-salt}} > \eta_{\text{K-salt}}$$

$$\chi_{\text{Li-salt}} > \chi_{\text{Na-salt}} > \chi_{\text{K-salt}} \text{ -aqueous phase}$$

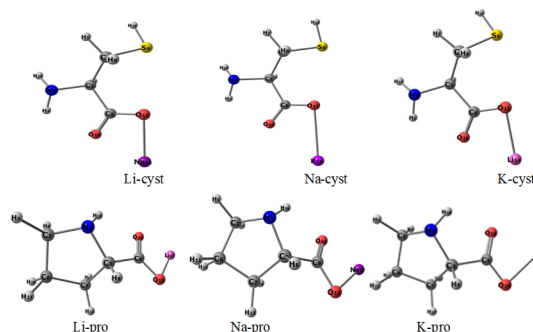


Fig. 2. Optimized structures for Li-cyst, Na-cyst, K-cyst, Li-pro, Na-pro and K-pro

Physical parameters viz. total dipole moment (TDM), HOMO-LUMO band gap energy (ΔE) and the C=O vibration in carboxylic group

In addition, the computed ΔE , TDM values, and C=O vibration of the carboxylic group of the investigated AAS in both gas and water phase. The two physical parameters TDM and E measure a given compound's reactivity^{22,23} and stability²⁴ with the molecules around it. Reactive chemicals are indicated by a high TDM and a low E ²⁵. From Li-AAS to Na-AAS and from Na-AAS to K-AAS, the total dipole moment increases while the band gap energy marginally lowers for both amino acids.

$$(\Delta E)_{\text{Li-salt}} > (\Delta E)_{\text{Na-salt}} > (\Delta E)_{\text{K-salt}},$$

$$(\text{TDM})_{\text{Li-salt}} < (\text{TDM})_{\text{Na-salt}} < (\text{TDM})_{\text{K-salt}},$$

$$\text{Aqueous phase (TDM and } \Delta E) > \text{Gas phase (TDM and } \Delta E)$$

Trend of total dipole moment (TDM) in both phase for AAS as shown below (TDM) pro-salts > (TDM) cyst-salts

Trend of HOMO/LUMO band gap energy (ΔE) in both phase for AAS as (ΔE) pro-salts < (ΔE) cyst-salts

The aforementioned trend clearly indicates that for the examined AAS, the TDM and E values are larger in aqueous solutions compared to gas phase. Fig. 3 and 4 present a graphic comparison of the E and TDM of Li-AAS, Na-AAS, and K-AAS, respectively. In both phases, it was discovered that K-pro had the lowest ΔE values, indicating that it was highly reactive, whereas Li-cyst had the highest ΔE values, indicating that it was the least reactive.

Due to an increase in the ionic radius of the metal ion, the C=O vibrational characteristic band of the carboxyl group was significantly shifted toward higher wavenumber from Li-AAS to Na-AAS and from Na-AAS to K-AAS. Observations show that K-pro has the highest and Li-pro has the lowest values.

Calculated Hydration Free Energies for all studied AAS molecules

Understanding the free energy of solvation, which is the energy required for a molecule to go from gas phase to solution, is essential for understanding how chemistry works in solutions. When water is the solvent, the term "solvation free energy" is often used to describe the hydration process. The hydration free energy²⁶ determines how stable an ion is in its hydrated state compared to how stable it is in its anhydrate condition. Hydration free energy was calculated using the DFT B3LYP method at the basis set of 6-31++G (d, p) (HFE), which is the work required to transfer a molecule from the gas phase into the solution phase. To calculate HFE, use the following equation.

$$\Delta G_{\text{Hydr}}^0 = \Delta G_{\text{s}}^0 - \Delta G_{\text{g}}^0$$

Where ΔG_{g}^0 and ΔG_{s}^0 represents the standard free energy of solute in the gas phase and in the solvent respectively, and ΔG_{Hydr}^0 refers as HFE. Table 4 and Fig. 5 compare the HFE of the interested AAS. HFE for all AAS under investigation is negative, indicating a strong solute-solvent interaction. Na-salts have greater HFE values than the corresponding Li- and K-salts for amino acids. Among the examined AAS, Na-cyst was shown to have the highest HFE values.

The observed trend for the HFE values for all studied AAS is (HFE) K-AAS (HFE) Li-AAS (HFE) Na-AAS

Table 1: Optimized geometrical parameters: (bond length (L) in Å and bond angle (A) in Deg.) for all studied AAS molecules obtained at B3LYP/6-311+G(d,p) level

Optimized geometrical parameters	Li-cyst	Na-cyst Gas Phase	K-cyst
L(O-M)	1.8610	2.1968	2.5537
A(O-C=O)	121.29	123.73	124.8
Aqueous Phase			
L(O-M)	2.0518	2.3561	2.7667
A(O-C=O)	122.71	124.33	125.27
Li-pro			
Gas Phase			
L(O-M)	1.8525	2.1956	2.5497
A(O-C=O)	120.92	123.43	124.47
Aqueous Phase			
L(O-M)	2.0251	2.3559	2.7597
A(O-C=O)	122.39	124.12	125.04

Table 2: Molecular properties viz. chemical hardness (η), softness (S), chemical potential (μ) and electronegativity (χ)

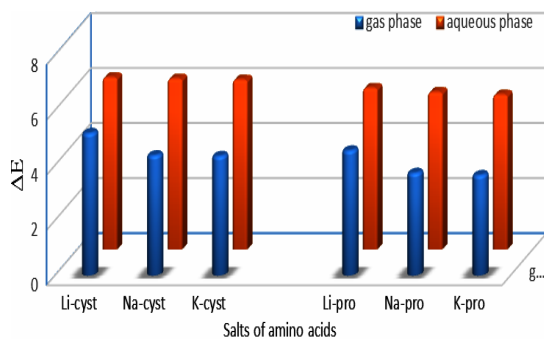
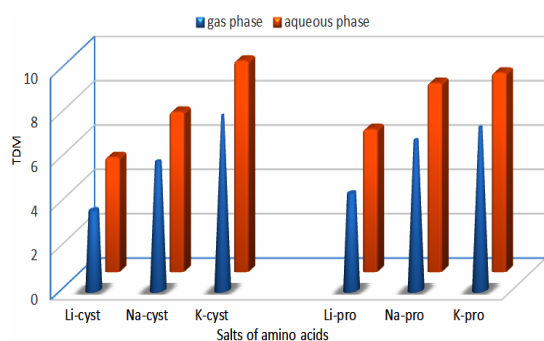
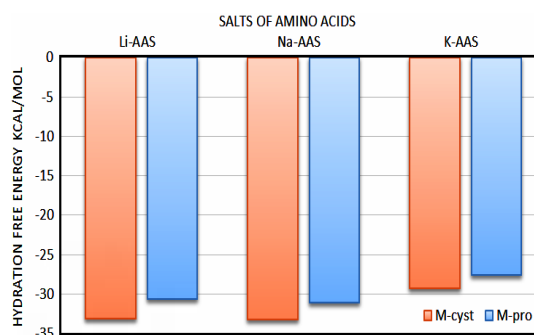
Molecular Properties	Li-cyst	Na-cyst Gas Phase	K-cyst
I	6.2706	5.9792	5.7648
A	1.1023	1.6183	1.4294
chemical hardness(η)	2.5842	2.1805	2.1677
softness (S)	0.3870	0.4586	0.4613
chemical potential(μ)	-3.6865	-3.7988	-3.5971
electronegativity(χ)	3.6865	3.7988	3.5971
Aqueous Phase			
I	6.6622	6.6266	6.5950
A	0.4060	0.4169	0.4229
chemical hardness(η)	3.1281	3.1049	3.0861
softness (S)	0.3197	0.3221	0.3240
chemical potential(μ)	-3.5341	-3.5218	-3.5090
electronegativity(χ)	3.5341	3.5218	3.5090
Li-pro			
Gas Phase			
I	5.6461	5.3313	5.0690
A	1.1083	1.6117	1.4278
chemical hardness(μ)	2.2689	1.8598	1.8206
softness (S)	0.4407	0.5377	0.5493
chemical potential(μ)	-3.3772	-3.4715	-3.2484
electronegativity(χ)	3.3772	3.4715	3.2484
Aqueous Phase			
I	6.1778	6.0715	6.0029
A	0.3056	0.3505	0.3752
chemical hardness(η)	2.9361	2.8605	2.8139
softness (S)	0.3406	0.3496	0.3554
chemical potential(μ)	-3.2417	-3.2110	-3.1891
electronegativity(χ)	3.2417	3.2110	3.1891

Table 3: Physical parameters for all studied AASviz. ΔE , TDM and the C=O vibration in carboxyl group

Molecular Properties	Li-cyst	Na-cyst	K-cyst
		Gas Phase	
ΔE (eV)	5.1683	4.3609	4.3354
TDM (D)	3.6075	5.8056	7.8980
C=O vibration	1580.3700	1592.5600	1601.5300
		Aqueous Phase	
ΔE (eV)	6.2562	6.2097	6.1721
TDM (D)	5.1733	7.2182	9.5197
C=O vibration	1573.3900	1577.5800	1582.1400
	Li-pro	Na-pro	K-pro
		Gas Phase	
ΔE (eV)	4.5378	3.7196	3.6412
TDM (D)	4.3832	6.7758	7.3595
C=O vibration	1567.7000	1587.5300	1600.4900
		Aqueous Phase	
ΔE (eV)	5.8722	5.7210	5.6277
TDM (D)	6.4383	8.5160	8.9823
C=O vibration	1571.4000	1579.2400	1584.3100

Table 4: Calculated Hydration Free Energies for all studied AAS molecules

Molecular Properties	Li-cyst	Na-cyst	K-cyst
Hydration Free Energy (Kcal/mol)	-33.08	-33.16	-29.26
	Li-pro	Na-pro	K-pro
Hydration Free Energy (Kcal/mol)	-30.66	-31.12	-27.52


Fig. 3. Comparison of ΔE of Li-cyst, Na-cyst, K-cyst, Li-pro, Na-pro and K-pro

Fig. 4. Comparison of TDM of Li-cyst, Na-cyst, K-cyst, Li-pro, Na-pro and K-pro

Fig. 5. Comparison of Hydration Free Energies of Li-cyst, Na-cyst, K-cyst, Li-pro, Na-pro and K-pro

CONCLUSION

As the O-M bond length increases from Li-AAS to Na-AAS and from Na-AAS to K-AAS with a change in the (C-O=C) bond angle, the geometry of the studied amino acid salt changes. All of the examined AAS experience an increase in and as they transition from a gaseous to an aqueous solution. It is known that both the aqueous phase and the gas phase of Li-cyst have the greatest η values. As a result, we can say that it is the least reactive. Both the TDM and ΔE varies as a result of increased size of metal and the alkyl part of studied amino acid. Lower ΔE and higher TDM values are the indicative of greater reactivity of K-AAS compare to Na-AAS. ΔE values of cyst-salt are higher than that of pro-salt. K-cyst has found to be highest dipole moment among all studied salts in both phases. The change in the geometrical parameters shifts C=O characteristic band toward lower wavenumbers. Negative value of the HFE of AAS suggests strong interaction between

AAS and water. The hydration free energy is highest for Na-AAS compare to Li-AAS and K-AAS.

Amravati and the Principal of the HPT Arts and RYK Science College in Nashik for providing research facilities and their kind cooperation.

ACKNOWLEDGEMENT

MBD thanks the Director of the Government Vidarbha Institute of Science and Humanities in

Conflicts of interest

Authors declares that there is no conflict of interest.

REFERENCES

- Zhang, Z.; Rao, S.; Han, Y.; Pang, R., and Ho, W. W. CO₂-selective membranes containing amino acid salts for CO₂/N₂ separation. *Journal of Membrane Science.*, **2021**, *638*, 119696.
- Liu, M., and Gadikota, G. Single-step, low temperature and integrated CO₂ capture and conversion using sodium glycinate to produce calcium carbonate. *Fuel.*, **2020**, *275*, 117887.
- Soroush, E.; Mesbah, M.; Hajilary, N., and Rezakazemi, M. ANFIS modeling for prediction of CO₂ solubility in potassium and sodium based amino acid Salt solutions. *Journal of Environmental Chemical Engineering.*, **2019**, *7*(1), 102925.
- M. J. Frisch.; G. W. Trucks.; H. B. Schlegel.; G. E. Scuseria.; M. A. Robb.; J. R. Cheeseman.; G. Scalmani.; V. Barone.; B. Mennucci.; G. A. Petersson.; H. Nakatsuji.; M. Caricato.; X. Li.; H. P. Hratchian.; A. F. Izmaylov.; J. Bloino.; G. Zheng.; J. L. Sonnenberg.; M. Hada.; M. Ehara.; K. Toyota.; R. Fukuda.; J. Hasegawa.; M. Ishida.; T. Nakajima.; Y. Honda.; O. Kitao.; H. Nakai.; T. Vreven.; J. A. Montgomery, Jr.; J. E. Peralta.; F. Ogliaro.; M. Bearpark, J. J. Heyd.; E. Brothers.; K. N. Kudin.; V. N. Staroverov.; T. Keith.; R. Kobayashi.; J. Normand.; K. Raghavachari.; A. Rendell, J. C. Burant.; S. S. Iyengar.; J. Tomasi.; M. Cossi.; N. Rega, J. M. Millam.; M. Klene, J. E. Knox.; J. B. Cross.; V. Bakken.; C. Adamo.; J. Jaramillo.; R. Gomperts.; R. E. Stratmann.; O. Yazyev.; A. J. Austin.; R. Cammi.; C. Pomelli.; J. W. Ochterski.; R. L. Martin.; K. Morokuma.; V. G. Zakrzewski.; G. A. Voth.; P. Salvador.; J. J. Dannenberg.; S. Dapprich.; A. D. Daniels.; O. Farkas.; J. B. Foresman.; J. V. Ortiz.; J. Cioslowski.; and D. J. Fox, Gaussian, Inc., Wallingford CT., **2013**.
- Tayade, K.; Bondhopadhyay, B.; Basu, A.; Chaitanya, G. K.; Sahoo, S. K.; Singh, N., & Kuwar, A. A novel urea-linked dipodal naphthalene-based fluorescent sensor for Hg (II) and its application in live cell imaging. *Talanta.*, **2014**, *122*, 16-22.
- Kaya, S.; Tüzün, B.; Kaya, C., & Obot, I. B. Determination of corrosion inhibition effects of amino acids: quantum chemical and molecular dynamic simulation study. *Journal of the Taiwan Institute of Chemical Engineers.*, **2016**, *58*, 528-535.
- Valaboju, A.; Gunturu, K. C.; Kotamarthi, B.; Joly, D., & Hissler, M. DFT study of Host-Dopant systems of DPVBi with Organophosphorus π -Conjugated materials. *Computational and Theoretical Chemistry.*, **2017**, *1113*, 61-71.
- Koopmans, T. Ordering of wave functions and eigenenergies to the individual electrons of an atom. *Physica.*, **1933**, *1*, 104-113.
- Zhang, G., & Musgrave, C. B. Comparison of DFT methods for molecular orbital eigenvalue calculations. *The Journal of Physical Chemistry A.*, **2007**, *111*(8), 1554-1561.
- Erdogan.; Safi, Z. S.; Kaya, S.; I in, D. O.; Guo, L., & Kaya, C. A computational study on corrosion inhibition performances of novel quinoline derivatives against the corrosion of iron. *Journal of Molecular Structure.*, **2017**, *1134*, 751-761.
- Miar, M.; Shiroudi, A.; Pourshamsian, K.; Olliaey, A. R., & Hatamjafari, F. Theoretical investigations on the HOMO–LUMO gap and global reactivity descriptor studies, natural bond orbital, and nucleus-independent chemical shifts analyses of 3-phenylbenzo [d] thiazole-2 (3 H)-imine and its para-substituted derivatives: Solvent and substituent effects. *Journal of Chemical Research.*, **2021**, *45*(1-2), 147-158.
- Choudhary, V.; Bhatt, A.; Dash, D., & Sharma, N. DFT calculations on molecular structures, HOMO–LUMO study, reactivity descriptors and spectral analyses of newly synthesized diorganotin (IV) 2 chloridophenylacetohydroxamate complexes. *Journal of computational chemistry.*, **2019**, *40*(27), 2354-2363.

13. Khan, S. A.; Rizwan, K.; Shahid, S.; Noamaan, M. A.; Rasheed, T., & Amjad, H. Synthesis, DFT, computational exploration of chemical reactivity, molecular docking studies of novel formazan metal complexes and their biological applications. *Applied Organometallic Chemistry.*, **2020**, *34*(3), e5444.
14. Pearson, R. G. **1997**. Chemical hardness, 10, No. 3527606173). Weinheim: Wiley-VCH.
15. Lucio, F. N. M.; da Silva, J. E.; Marinho, E. M.; Mendes, F. R. D. S.; Marinho, M. M., & Marinho, E. S. Methylcytosine alcaloid potentially active against dengue virus: a molecular docking study and electronic structural characterization. *Int J Res.*, **2020**, *8*(1), 221-36.
16. Ibrahim, M. Molecular modeling and FTIR study for K, Na, Ca and Mg coordination with organic acid. *Journal of Computational and Theoretical Nanoscience.*, **2009**, *6*(3), 682-685.
17. Abad, N.; Hajji, M.; Ramli, Y.; Belkhiria, M.; Mofteh H. Elmgirhi, S.; A. Habib, M., & Essassi, E. M. A newly synthesized nitrogen rich derivative of bicyclic quinoxaline-Structural and conceptual DFT reactivity study. *Journal of Physical Organic Chemistry.*, **2020**, *33*(6), e4055.
18. Chakraborty, D., & Chattaraj, P. K. Conceptual density functional theory based electronic structure principles. *Chemical Science.*, **2021**, *12*(18), 6264-6279.
19. Mebi, C. A. DFT study on structure, electronic properties, and reactivity of cis-isomers of $[(NC_5H_4-S)_2Fe(CO)_2]$. *Journal of Chemical Sciences.*, **2011**, *123*(5), 727-731.
20. Makov, G. Chemical hardness in density functional theory. *The Journal of Physical Chemistry.*, **1995**, *99*(23), 9337-9339.
21. Dheivamalar, S., & Banu, K. B. A DFT study on functionalization of acrolein on Ni-doped (ZnO) 6 nanocluster in dye-sensitized solar cells. *Heliyon.*, **2019**, *5*(12), e02903.
22. Ibrahim, M., & Mahmoud, A. A. Computational notes on the reactivity of some functional groups. *Journal of Computational and Theoretical Nanoscience.*, **2009**, *6*(7), 1523-1526.
23. Ezzat, H. A.; Hegazy, M. A.; Nada, N. A.; & Ibrahim, M. A. Effect of nano metal oxides on the electronic properties of cellulose, chitosan and sodium alginate. *Biointerface Res. Appl. Chem.*, **2019**, *9*, 4143-4149.
24. Singh, J. S. IR and Raman spectra with Gaussian-09 molecular analysis of some other parameters and vibrational spectra of 5-fluoro-uracil. *Research on Chemical Intermediates.*, **2020**, *46*(5), 2457-2479.
25. Miar, M.; Shiroudi, A.; Pourshamsian, K.; Oliaey, A. R., & Hatamjafari, F. Theoretical investigations on the HOMO-LUMO gap and global reactivity descriptor studies, natural bond orbital, and nucleus-independent chemical shifts analyses of 3-phenylbenzo [d] thiazole-2 (3 H)-imine and its para-substituted derivatives: Solvent and substituent effects. *Journal of Chemical Research.*, **2021**, *45*(1-2), 147-158.
26. Tansel, B. Significance of thermodynamic and physical characteristics on permeation of ions during membrane separation: Hydrated radius, hydration free energy and viscous effects. *Separation and Purification Technology.*, **2012**, *86*, 119-126.